Journal of Balkan Science and Technology
journal homepage: www.jbst.nku.edu.tr/

The Hirshfeld Surface Analysis of Antimony(III) and Bismuth(III) Complexes with Dithiocarbamate Ligands

Ibrahim Ismet OZTURK[1], Okan UÇAR[1,2*]

[1]*Section of Inorganic Chemistry, Department of Chemistry, Tekirdag Namık Kemal University, 59030, Tekirdag, Türkiye*
[2]*Section of Analytical Chemistry, Department of Chemistry, Yozgat Bozok University, 66100, Yozgat, Türkiye*

Research Article

Keywords:
Antimony(III) halides
Bismuth(III) halides
Dithiocarbamates
Hirshfeld Surface Analysis
Intermolecular interactions

Received: 22.06.2022
Accepted: 01.08.2022
Published:14.09.2022

DOI: 10.55848/jbst.2022.12

ABSTRACT

The Hirshfeld surface analysis represents one of the most effective ways to determine intermolecular interactions in a crystal. Using the Hirshfeld surface analysis, both the types and quantities of these interactions can be determined. In this study, intermolecular interactions of [1] (**1**), {[SbBr(Me_2DTC)$_2$]$_n$} (**2**), {[SbI(Me_2DTC)$_2$]$_n$} (**3**), {[SbI(Et_2DTC)$_2$]$_2$} (**4**), {[BiCl(Me_2DTC)$_2$]$_n$}(**5**), {[BiBr(Me_2DTC)$_2$]$_n$} (**6**), {[BiBr$_2$(Et_2DTC)]$_n$} (**7**), {[BiI$_2$(Me_2DTC)$_n$]} (**8**) and {[BiI(Et_2DTC)$_2$]$_n$} (**9**) (Me_2DTC: Dimethyldithiocarbamate, Et_2DTC: Diethyldithiocarbamate), previously synthesized and characterized by different spectroscopic methods and X-ray diffraction in literature, were determined by using the Hirshfeld surface analysis. The Hirshfeld surface analysis was carried out via Crystal Explorer 21.5. The results of the Hirshfeld surface analysis show that the highest contributions to the crystal packing of the complexes **1**-**9** are H···H, S···H/H···S and X···H/H···X (X: Cl, Br and I). The contribution of X···S/S···X and M···X/X···M (M: Sb and Bi) interactions is higher in bismuth (III) complexes as compared to antimony (III) complexes.

1. Introduction

Antimony and bismuth, which are in Group 15 of the periodic table, have been known since ancient times [1]. These group elements are more stable in trivalence and contain a lone electron pair [2]. Antimony(III) and bismuth(III) complexes with ligands containing sulfur donor atoms have been synthesized previously in the literature [3-5]. Both lone electron pair and secondary interactions (M···S or M···X, X: Cl, Br, I) lead to various coordination numbers and molecular geometries [6]. Antimony and bismuth compounds are also biologically important. Antimonial drugs are used for the treatment of Leishmaniasis, whereas bismuth compounds have been used against various microbial diseases for many years [7, 8]. In addition, both antimony(III) and bismuth(III) halide complexes with dithiocarbamates have been shown higher antitumor activity than cisplatin and doxorubicin (anticancer agents). Non-covalent interactions have significant impacts on coordination chemistry and biological activities. In addition, these interactions affect the stability of the crystal [9]. These interactions can be determined by using the Hirshfeld surface analysis. Hirshfeld surfaces mapped with dnorm visually present significant intermolecular interactions between atoms in compounds with red dots. Two-dimensional fingerprints provide information about the contributions of non-covalent interactions to the hirshfeld surfaces[10].

In this work, the compounds {[SbCl(Me_2DTC)$_2$]$_n$} (**1**), {[SbBr(Me_2DTC)$_2$]$_n$} (**2**), {[SbI(Me_2DTC)$_2$]$_n$} (**3**), {[SbI(Et_2DTC)$_2$]$_2$}(**4**), {[BiCl(Me_2DTC)$_2$]$_n$}(**5**), {[BiBr(Me_2DTC)$_2$]$_n$} (**6**), {[BiBr$_2$(Et_2DTC)]$_n$} (**7**), {[BiI$_2$(Me_2DTC)$_n$]} (**8**), and {[BiI(Et_2DTC)$_2$]$_n$} (**9**), previously synthesized and characterized in the literature, were selected [11–14] . The crystal structures of complexes **1**-**9** were determined by X-ray diffraction (Fig 1.). The intermolecular contacts of the complexes **1**-**9** were examined by the Hirshfeld surface analysis and by using Crystal Explorer ver. 21.5.

2. Materials and Methods

The hirshfeld surface analysis[11]] was used to visualize the intermolecular interactions of the antimony(III) and bismuth (III)-dithiocarbamate complexes [12-15]. Hirshfeld surface, fingerprint plots [16] were generated using Crystal Explorer Program ver. 21.5 program based on the input CIF files [17]. Two parameters are defined on all hirshfeld surfaces: d_i (the distance to the nearest surface inside) and d_e (the distance to the nearest surface outside). d_{norm}, the normalized contact distance can be given by the following equation:

$$d_{norm}\frac{d_i - r_i^{vdw}}{r_i^{vdw}} + \frac{d_e - r_e^{vdw}}{r_e^{vdw}}$$

r_i^{vdw} and r_e^{vdw} correspond to the van der Waals radii of the atoms. The red, white and blue spots are seen on the d_{norm} surface according to short, equal and long interactions, respectively.The 2D fingerprints gave depending on d_e and d_i list the interactions in a crystal structure. The quantitative value of each interaction can be obtained from fingerprint plots.

* Corresponding author: *Section of Analytical Chemistry, Department of Chemistry, Yozgat Bozok University, 66100, Yozgat, Türkiye*
E-mail addresses: okan.ucar@bozok.edu.tr

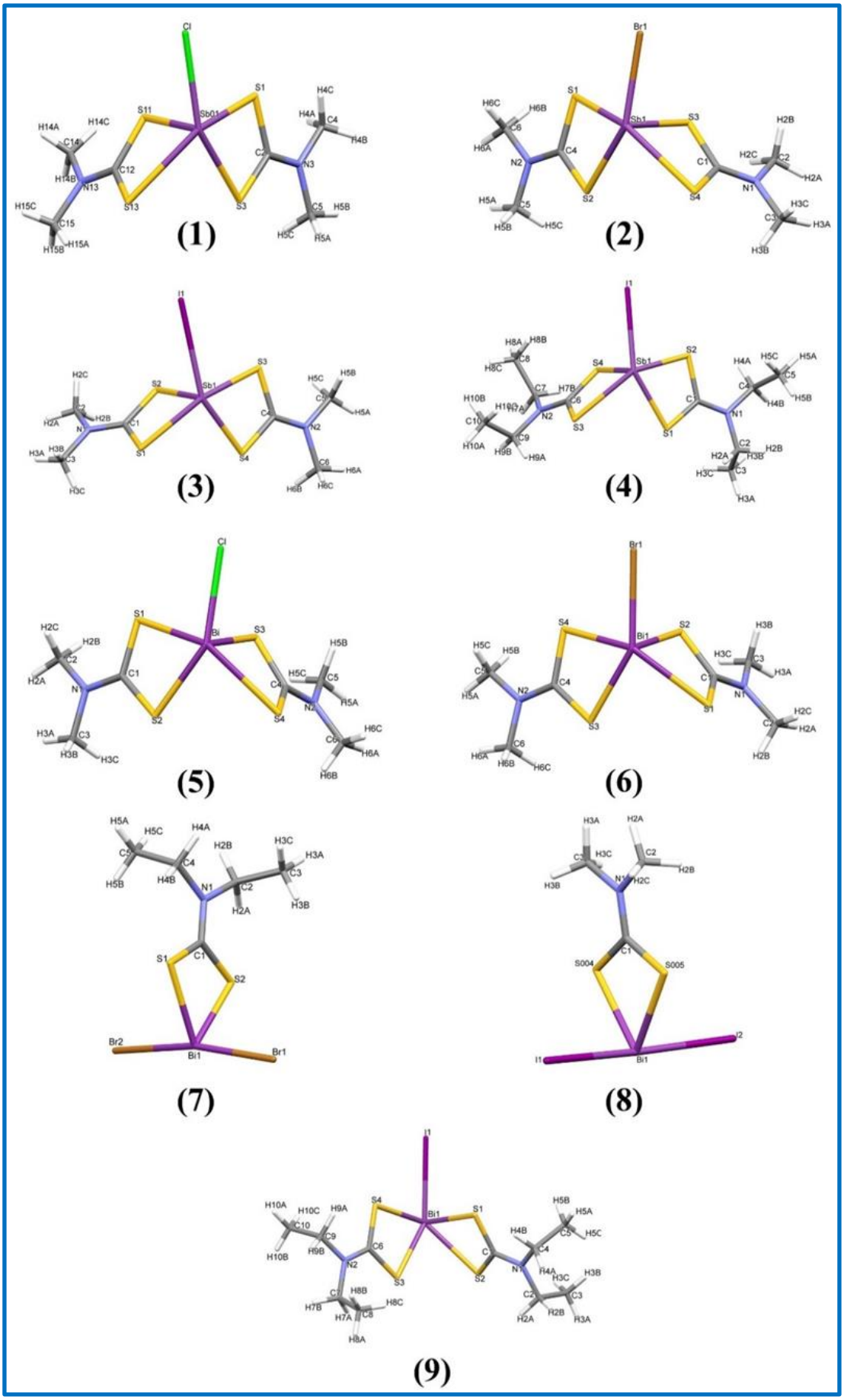

Fig. 1 The crystal structures of complexes **1**-**9**.

3. Results and Discussion

Non-covalent interactions are important in the formation of a crystal [18]. The Hirshfeld surface analysis is a tool used to understand intermolecular interactions in a crystal [19]. All Hirschfeld surfaces were determined for the complexes 1-9. The dnorm, di and de mapped molecular hirshfeld surfaces of the antimony(III) complexes **1-4** are shown in table. 1 and fig 2. d_{norm} ranges of the complexes 1-4 are -0.3101 Å to 1.2128, Å -0.1544 Å to 1.0947 Å, -0.2437 Å to 1.2218 Å, -0.1780 Å to 1.1675 Å, respectively. The red dots on the d_{norm} map provide information about the distance of the contacts. Contacts shorter than the van der Waals radii appear as red rings, while distant contacts seem as blue surfaces. The most intense red dots on the d_{norm} surface are Sb···Cl/Cl···Sb interactions for complex **1**. Intermolecular μ_2-S···Sb/Sb···μ_2-S interactions leading to polymerization of complex **1** achieve pale spots on the d_{norm} surface. Also, other pale red spots on the dnorm surface of complex **1** show C-H···S and C-H···Cl type intermolecular hydrogen bonds. The darkest red on the d_{norm} surface are Sb···S/S···Sb contacts for complex **2** and these contacts form polymerization with μ_2-S among monomeric units. H···S/S···H (C-H···S type intermolecular hydrogen bond) interactions between monomeric units create light red rings on the dnorm surface. In complexes **3** and **4**, Sb···I/I···Sb interactions are shorter than the sum of antimony and iodide van der Waals radii. Thus, a dark red ring is formed on the dnorm map. The pale red spots on the d_{norm} surface indicate C-H···S, C-H···C and C-H···I type intermolecular hydrogen bonds for complex **3** and C-H···S type intermolecular hydrogen bond for complex **4**.

The d_{norm}, di and de mapped molecular hirshfeld surfaces of the bismuth(III) complexes **5-9** are shown in Fig. 3. d_{norm} ranges of the complexes **5-9** are -0.4015 Å to 1.0795 Å, -0.3769 Å to 1.1967 Å, -0.4356 Å to 1.1552 Å, -0.3512 Å to 1.5052 Å, -0.3241 Å to 1.4078 Å, respectively. The most intense red dots on the d_{norm} surface are Bi···Cl/Cl···Bi (intermolecular μ_2-Cl···Bi interactions leading to polymerization) interactions for complex **5**. Many pale red spots exist on the d_{norm} surface caused by C-H···S, C-H···C and C-H···Cl type intermolecular hydrogen bonds and S···N/N···S, H···H and S···C/C···S contacts. The most intense red dots on the d_{norm} surface are Bi···Br/Br···Bi (intermolecular μ_2-Br···Bi interactions leading to polymerization) interactions for complex **6**. Many pale red spots exist on the d_{norm} surface caused C-H···S, C-H···C and C-H···Br type intermolecular hydrogen bonds and S···N/N···S, Bi···S/S···Bi, H···H and S···C/C···S contacts. The most intense red dots on the d_{norm} surface are Bi···Br/Br···Bi and Bi···S/S···Bi (intermolecular μ_2-Br···Bi and μ_2-S···Bi interactions leading to polymerization) interactions for complex **7**. The pale red spots exist on the d_{norm} surface caused C-H···Br type intermolecular hydrogen bond. The most intense red dots on the dnorm surface are Bi···I/I···Bi (intermolecular μ_2-I···Bi interactions leading to polymerization) interactions for complex **8**. The pale red spots exist on the d_{norm} surface as caused C-H···I, C-H···N and C-H···C type intermolecular hydrogen bond and I···S/S···I contacts. The most intense red dots on the d_{norm} surface are Bi···I/I···Bi and Bi···S/S···Bi (intermolecular μ_2-I···Bi and μ_2-S···Bi interactions leading to polymerization) interactions for complex **9**. The pale red spots exist on the d_{norm} surface caused C-H···S and C-H···C type intermolecular hydrogen bonds and H···H contact.

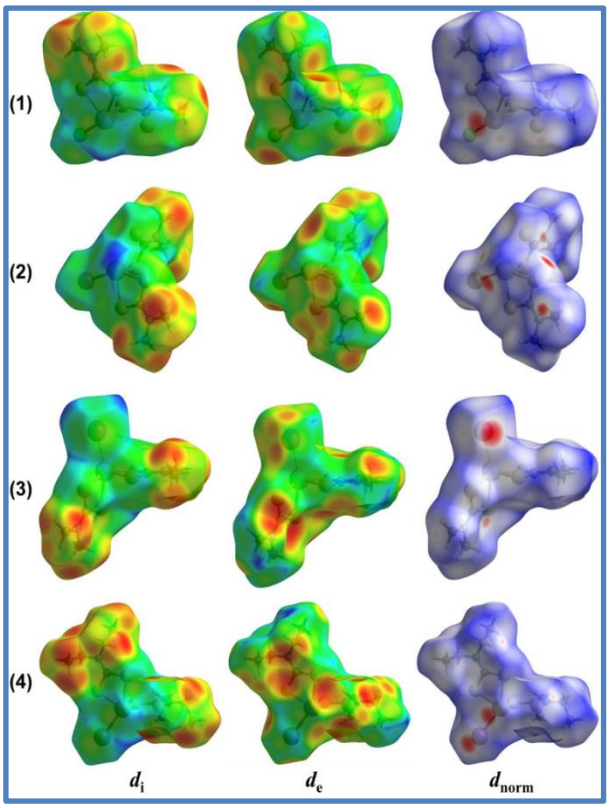

Fig. 2 Hirshfeld surfaces mapped with di (interior distance), de (exterior distance) and dnorm (normalized contact distance) in antimony(III) halide complexes **1-4**.

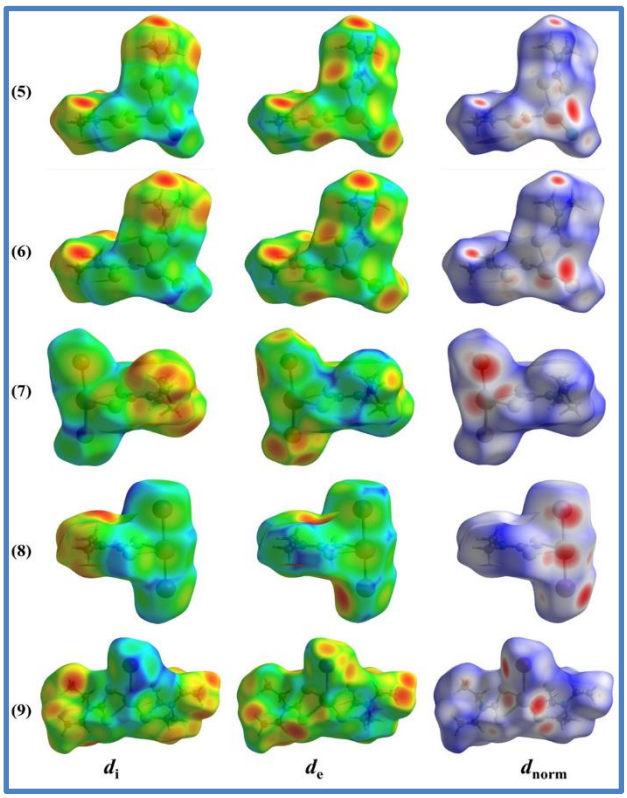

Fig. 3 Hirshfeld surfaces mapped with d_i (interior distance), d_e (exterior distance) and d_{norm} (normalized contact distance) in bismuth(III) halide complexes **5-9**.

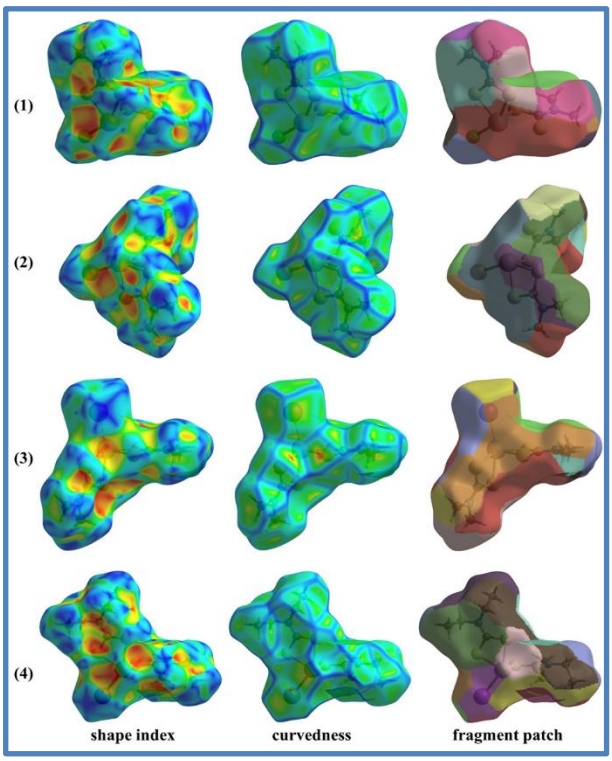

Fig. 4 Hirshfeld surfaces mapped with shape index, curvedness and fragment patch in antimony(III) halide complexes 1-4.

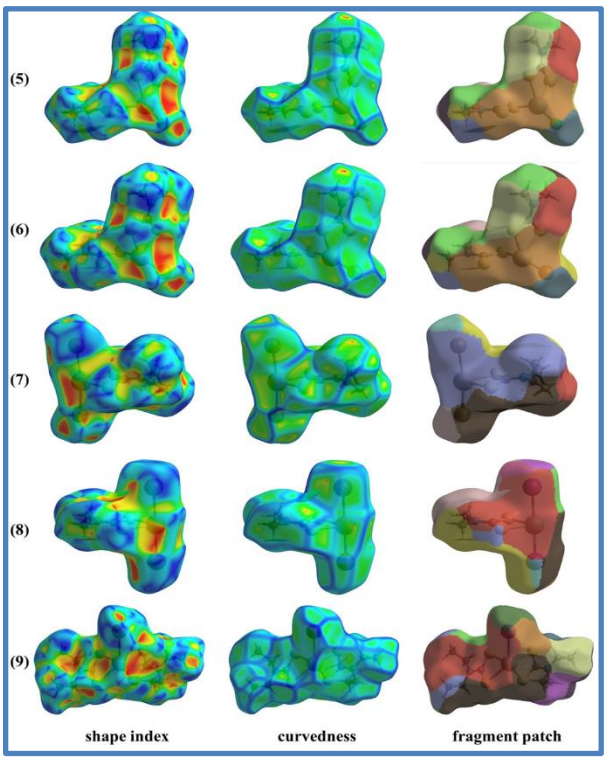

Fig. 5. Hirshfeld surfaces mapped with shape index, curvedness and fragment patch in bismuth(III) halide complexes 5-9.

Hirshfeld surface mapped of shape index, curvedness and fragment patch in complexes 1-9 have shown in Fig. 4 and Fig.5. Shape index and curvedness have been mapped over the ranges −1.0 to 1.0 Å and −4.0 to 0.4 Å, respectively. The red regions in the shape index represent the hollows in the crystal, while the blue regions correspond to the humps. Stacking resulting from π-π interaction in crystal structures appears as red and blue triangles on shape index maps. The absence of red and blue triangles in the shape indices of the complexes is evidence that there is no π-π interaction. The yellow and red dots on the curvedness maps indicate strong hydrogen bonds.

The fingerprint plots show the contributions of contacts between various atoms to the formation of the Hirshfeld surface. In these graphics, the percentage contribution of the A···B/B···A interaction theme is given. The x and y axes of this graph consist of d_i and d_e, respectively. The blue area in the graph represents the contribution of the A···B/B···A interaction, while the grey area represents the total contribution in the crystal. The fingerprint plots of complexes **1-4** are present in Fig. 6. The strongest interaction in complex 1 is H···H with 35.0%. Then, S···H/H···S (26.7%), Cl···H/H···Cl (15.0%) and C···H/H···C (4.7%) interactions are listed. S···H/H···S and Cl···H/H···Cl contacts seem two sharp spikes at their fingerprint plots. In complex **2**, S···H/H···S is the highest interaction with a 31.2% contribution. The other significant contributions are H···H (29.9%), Br···H/H···Br (18.4%), C···H/H···C (5.6%) and Sb···S/S···Sb (5.6%) interactions. S···H/H···S and Br···H/H···Br interactions form in two symmetrical sharp spikes. The major additive to the Hirshfeld surface area for complex **3** is from H···H contacts (28.5%). The next most significant contribution with 27.8% of the overall surface is S···H/H···S interaction and it has two spikes. The extents of I···H/H···I (18.7%) and S···S (6.1%) interactions comprise the Hirshfeld surface of complex 3. The most important contact is H···H interaction in complex 4. Its contribution has a value of 41.1%. The second most significant contact is S···H/H···S with 28.4% and this contact appear as two sharp spikes in the fingerprint plot. I···H/H···I and C···H/H···C interactions align with 16.8% and 4.8%, respectively.

The fingerprint plots of complexes **5-9** are present in Fig. 7. In complex **5**, H···H contact is the most common interaction with 35.0%. S···H/H···S and Cl···H/H···Cl (with two sharp spikes) contacts have important contributions with 26.1% and 14.2% in crystal. Complex **6** is dominated by H···H (34.5%) interaction. Further, S···H/H···S (26.4%) and Br···H/H···Br (14.8%) are the contribution of other considerable interactions. The highest interaction of crystal packing in complex **7** is Br···H/H···Br (39.9%) contact. H···H (22.2%) and S···H/H···S (17.6%) interactions come after the Br···H/H···Br. The Br···H/H···Br and S···H/H···S appear in two sharp spikes in their fingerprint plots. The majority of interactions in complex **8** is of I···H/H···I (30.2%) contacts. The S···H/H···S (18.2%) interactions show the second highest contact in the crystal. Unlike other molecules, the Bi···I/I···Bi interaction has an important contribution with 15.9%. A huge 49.4% contribution of the H···H contact to the packing of the crystal takes attention in complex **9**. The next contribution is S···H/H···S with 17.9%. The third is I···H/H···I (14.5%) contacts. All contact contributions of complexes **1-9** are summarized in Tables 1 and 2.

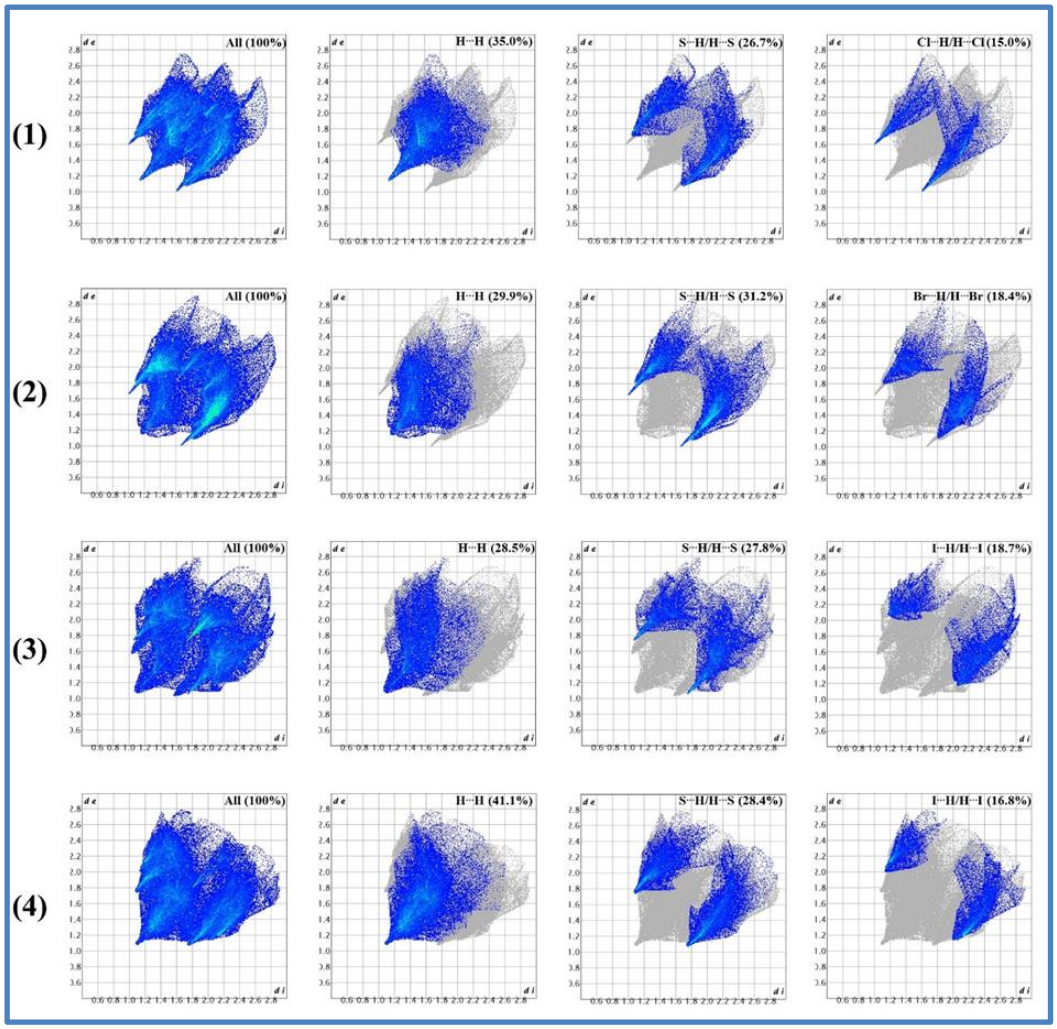

Fig. 6 2D fingerprint plots and percentage contributions to the total Hirshfeld surface of antimony(III) halide complexes **1-4**, All, H···H, S···H/H···S, and X···H/H···X, respectively.

Table 1. The contact contributions to the Hirshfeld surface in antimony(III) halide complexes **1-4**.

Interactions	Complex 1 (X: Cl)	Complex 2 (X: Br)	Complex 3 (X: I)	Complex 4 (X: I)
H···H	35.0	29.9	28.5	41.1
S···H/H···S	26.7	31.2	27.8	28.4
X···H/H···X	15.0	18.4	18.7	16.8
X···X	0.2	-	-	0.4
S···S	2.8	1.5	6.1	0.9
N···N	-	0.2	-	-
X···N/N···X	-	0.4	0.4	-
X···S/S···X	2.0	3.1	2.6	0.4
X···C/C···X	-	-	0.7	-
S···C/C···S	2.1	-	-	-
S···N/N···S	0.8	0.4	0.9	-
C···H/H···C	4.7	5.6	5.9	4.8
N···H/H···N	2.0	0.8	1.5	1.2
N···C/C···N	-	0.2	-	-
Sb···X/X···Sb	3.5	0.2	2.3	2.3
Sb···H/H···Sb	0.7	2.7	4.6	3.7
Sb···S/S···Sb	4.5	5.6	-	-
TOTAL	**100.0**	**100.0**	**100.0**	**100.0**

Table 2. The contact contributions to the Hirshfeld surface in bismuth(III) halide complexes **5-9**

Interactions	Complex 5 (X: Cl)	Complex 6 (X: Br)	Complex 7 (X: Br)	Complex 8 (X: I)	Complex 9 (X: I)
H···H	35.0	34.5	22.2	12.4	49.4
S···H/H···S	26.1	26.4	17.6	18.2	17.9
X···H/H···X	14.2	14.8	39.9	30.2	14.5
X···X	0.2	0.3	0.6	7.6	-
S···S	3.3	3.0	-	2.6	2.9
Bi···Bi	-	-	0.1	0.1	-
X···N/N···X	-	-	-	-	0.1
X···S/S···X	2.0	2.0	4.6	6.6	1.4
X···C/C···X	0.3	0.6	-	-	0.8
S···C/C···S	1.9	2.0	-	-	1.2
S···N/N···S	0.7	0.7	0.3	-	0.1
C···H/H···C	4.6	4.1	1.9	4.1	2.4
N···H/H···N	1.9	1.9	0.2	2.0	1.2
Bi···X/X···Bi	3.7	3.7	8.0	15.9	3.5
Bi···C/C···Bi	-	-	-	-	0.4
Bi···H/H···Sb	0.8	0.7	0.9	0.1	1.4
Bi···S/S···Bi	5.3	5.3	3.7	-	2.8
TOTAL	**100.0**	**100.0**	**100.0**	**100.0**	**100.0**

4. Conclusion

The Hirshfeld surface analyzes of dithiocarbamate derivative ligands antimony(III) and bismuth(III) halide complexes, which are synthesized and characterized with various spectroscopic methods and X-ray diffraction, have been studied. It has been determined that the short interactions in bismuth(III) complexes on dnorm surfaces are more than in antimony(III) complexes. Intermolecular interactions constitute one of the factors affecting biological activity. In the literature, it has been stated that low H-all intermolecular interactions in these complexes **1-9** increase the biological activity. The quantities of H-all intermolecular interactions obtained from the two-dimensional fingerprints of the complexes support this situation.

In the crystal packing of complexes **1-9**, it has been determined that using the Hirshfeld surface analysis, H···H, S···H/H···S and X···H/H···X (X: Cl, Br or I) interactions have, in general, higher percentages (Fig 8and Fig 9). In complexes **4** and **9**, H···H interaction is greater because there are more hydrogen atoms in their structures. In addition, since the number of hydrogen atoms in complex **8** is less than in other complexes, the percentage of H···H interaction is relatively lower. In compounds **1**, **3-6**, and **9** the H···H interaction is the most dominant. In compounds **7** and **8**, the H–H contacts contribute the most to the total Hirshfeld surface area. Only in complex **2**,

S···H/H···S interaction has the highest contribution to crystal packing. In addition, Bi···X/X···Bi interactions in complexes **7** and **8** in 1:1 molar stoichiometric ratios prompt important contributions.

Declaration

Author Contribution: Conceive-I.I.O., O.U.; Design-I.I.O., O.U.; Supervision-I.I.O., O.U.; Experimental Performance, Data Collection and/or Processing-I.I.O., O.U.; Analysis and/or Interpretation- I.I.O., O.U.; Literature Review-I.I.O., O.U.; Writer- I.I.O., O.U.; Critical Reviews– I.I.O., O.U.

Conflict of interests: The author has declared no conflicts of interest.

Orcid-ID

İbrahim İsmet Öztürk https://orcid.org/0000-0003-3164-0038
Okan Uçar https://orcid.org/0000-0001-5921-3324

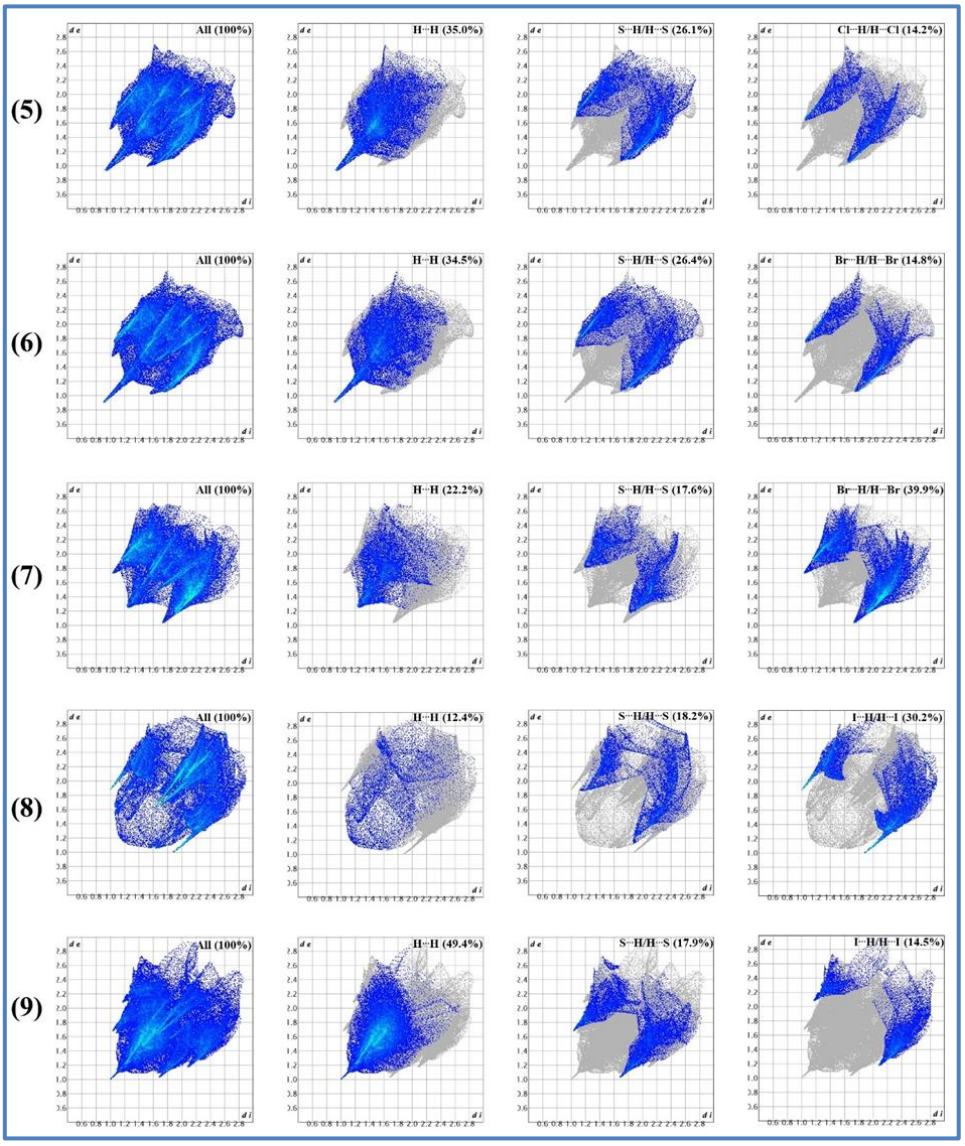

Fig. 7 2D fingerprint plots and percentage contributions to the total Hirshfeld surface of bismuth(III) halide complexes **5-9**, All, H···H, S···H/H···S, and X···H/H···X, respectively.

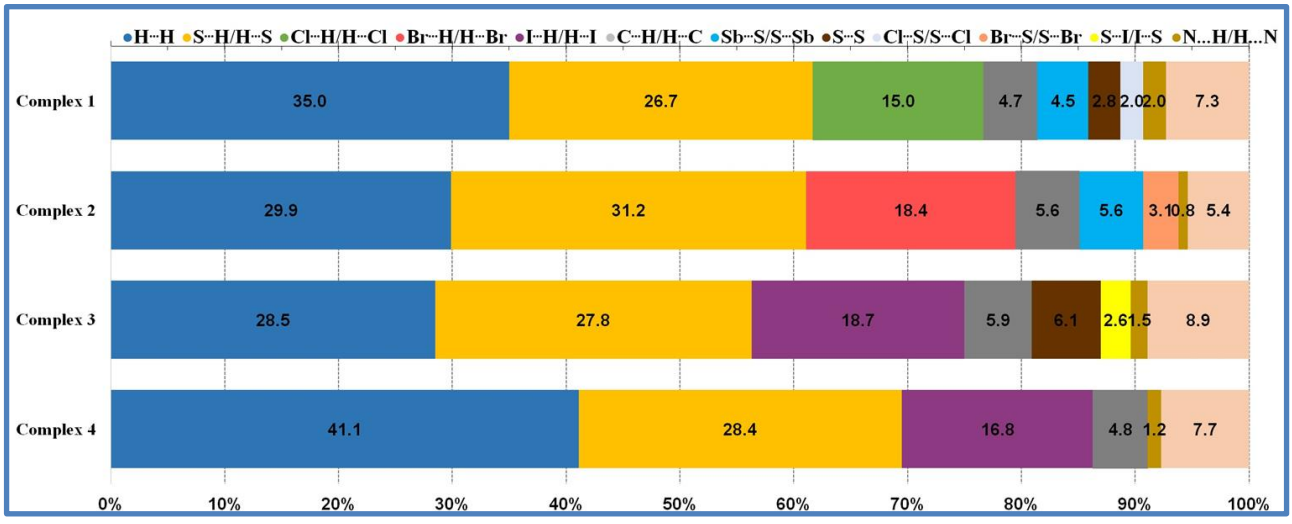

Fig. 8 Relative contributions of intermolecular interactions to the Hirshfeld surface area for antimony(III) halide complexes **1-4.**

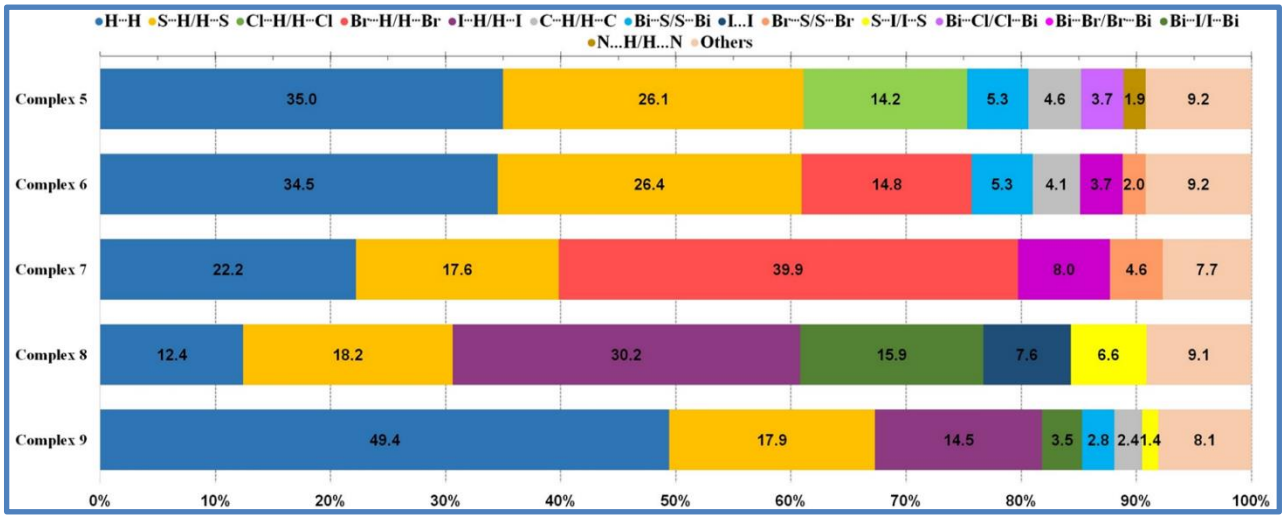

Fig. 9 Relative contributions of intermolecular interactions to the Hirshfeld surface area for bismuth(III) halide complexes **5-9**.

References

[1] K. S. Ferraz *et al.*, "Investigation on the pharmacological profile of 2,6-diacetylpyridine bis(benzoylhydrazone) derivatives and their antimony(III) and bismuth(III) complexes," (in eng), *Eur J Med Chem*, vol. 53, pp. 98-106, Jul 2012, doi: 10.1016/j.ejmech.2012.03.040.

[2] E. I. Davydova, A. Virovets, E. Peresypkina, A. V. Pomogaeva, and A. Y. Timoshkin, "Crystal structures of antimony(III) chloride complexes with pyridine," *Polyhedron*, vol. 158, pp. 97-101, 2019/01/15/ 2019, doi: https://doi.org/10.1016/j.poly.2018.10.056.

[3] S. Yarar *et al.*, "Synthesis, characterization and cytotoxic properties of bismuth(III) chloride complexes with heterocyclic thioamides," *Inorganica Chimica Acta*, vol. 471, pp. 23-33, 2018/02/24/ 2018, doi: https://doi.org/10.1016/j.ica.2017.10.026.

[4] O. Ucar, A. M. Grześkiewicz, C. Banti, S. K. Hadjikakou, and I. I. Ozturk, "Structural characterization and biological evaluation of antimony(III) and bismuth(III) complexes with imidazolidine-2-thione," *Journal of Molecular Structure*, vol. 1235, p. 130270, 2021/07/05/ 2021, doi: https://doi.org/10.1016/j.molstruc.2021.130270.

[5] I. I. Ozturk *et al.*, "Synthesis, characterization and biological evaluation of novel antimony(III) iodide complexes with tetramethylthiourea and N-ethylthiourea," *Inorganica Chimica Acta*, vol. 491, pp. 14-24, 2019/06/01/ 2019, doi: https://doi.org/10.1016/j.ica.2019.03.020.

[6] Ozturk, II *et al.*, "Synthesis, characterization and biological studies of new antimony(III) halide complexes with ω-thiocaprolactam," (in eng), *J Inorg Biochem*, vol. 109, pp. 57-65, Apr 2012, doi: 10.1016/j.jinorgbio.2012.01.014.

[7] S. Yan, F. Li, K. Ding, and H. Sun, "Reduction of pentavalent antimony by trypanothione and formation of a binary and ternary complex of antimony(III) and trypanothione," *JBIC Journal of Biological Inorganic Chemistry*, vol. 8, no. 6, pp. 689-697, 2003/07/01 2003, doi: 10.1007/s00775-003-0468-1.

[8] V. Venkatachalam, K. Ramalingam, U. Casellato, and R. Graziani, "Structural and electronic effects of alkyl substituents on the main group dithiocarbamato complexes: crystal and molecular structures of tris(N,N′-iminodiethanoldithiocarbamato)metal(III) complexes (M As, Sb and Bi) and cyclic voltammetric studies on substituted dithiocarbamates," *Polyhedron*, vol. 16, no. 7, pp. 1211-1221, 1997/01/01/ 1997, doi: https://doi.org/10.1016/S0277-5387(96)00362-2.

[9] M. Spackman and J. McKinnon, "Fingerprinting Intermolecular Interactions in Molecular Crystals," *CrystEngComm*, vol. 4, pp. 378-392, 08/01 2002, doi: 10.1039/B203191B.

[10] A. Radha *et al.*, "An insight into non-covalent interactions in the tetraphenylarsonium dithiophosphates: Synthesis, DFT and Hirshfeld surface analysis," *Journal of Molecular Structure*, vol. 1229, p. 129729, 2021/04/05/ 2021, doi: https://doi.org/10.1016/j.molstruc.2020.129729.

[11] M. A. Spackman and D. Jayatilaka, "Hirshfeld surface analysis," *CrystEngComm*, 10.1039/B818330A vol. 11, no. 1, pp. 19-32, 2009, doi: 10.1039/B818330A.

[12] M. Arda *et al.*, "Novel bismuth compounds: synthesis, characterization and biological activity against human adenocarcinoma cells," *Rsc Advances*, vol. 6, no. 35, pp. 29026-29044, 2016.

[13] O. S. Urgut *et al.*, "New antimony(III) halide complexes with dithiocarbamate ligands derived from thiuram degradation: The effect of the molecule's close contacts on in vitro cytotoxic activity," *Materials Science and Engineering: C*, vol. 58, pp. 396-408, 2016/01/01/ 2016, doi: https://doi.org/10.1016/j.msec.2015.08.030.

[14] I. Ozturk *et al.*, "Synthesis, characterization and biological activity of antimony(III) or bismuth(III)

chloride complexes with dithiocarbamate ligands derived from thiuram degradation," *Polyhedron*, vol. 67, pp. 89–103, 01/08 2014, doi: 10.1016/j.poly.2013.08.052.

[15] O. S. Urgut *et al.*, "Addition of tetraethylthiuram disulfide to antimony(III) iodide; synthesis, characterization and biological activity," *Inorganica Chimica Acta*, vol. 443, pp. 141-150, 2016/03/24/ 2016, doi: https://doi.org/10.1016/j.ica.2015.12.028.

[16] J. J. McKinnon, D. Jayatilaka, and M. A. Spackman, "Towards quantitative analysis of intermolecular interactions with Hirshfeld surfaces," *Chemical Communications*, 10.1039/B704980C no. 37, pp. 3814-3816, 2007, doi: 10.1039/B704980C.

[17] M. Turner *et al.*, "CrystalExplorer17," ed: The University of Western Australia Australia, 2017.

[18] D. Braga and F. Grepioni, "Intermolecular interactions in nonorganic crystal engineering," *Accounts of chemical research*, vol. 33, no. 9, pp. 601-608, 2000.

[19] M. E. Ghali, Z. Aloui, I. Hassini, S. Akriche, and M. Rzaigui, "Synthesis, crystal structure, Hirshfeld surface analysis, optical and antioxidant properties of the binuclear complex [C5H14N2]2Bi2Br10.4H2O," *Journal of Molecular Structure*, vol. 1226, p. 129252, 2021/02/15/ 2021, doi: https://doi.org/10.1016/j.molstruc.2020.129252.